Fatigue crack micromechanisms on a PE Zn-Cu-Al alloy

Vittorio Di Cocco, Francesco Iacoviello
Università di Cassino e del Lazio Meridionale, DiCeM, via G. Di Biasio 43, 03043 Cassino (FR), Italy
v.dicocco@unicas.it

Stefano Natali, Valerio Volpe
Università di Roma "La Sapienza", DICMA, via Eudossiana 18, Rome, Italy

Francesco Maiolino
Seconda Università di Napoli , DAeDI via S.Lorenzo 81031 Aversa (CE) , Italy

ABSTRACT. Some Cu-Zn-Al alloy is able to exhibit an important feature: the Pseudo-Elastic behavior, commonly defined as PE alloy. The PE effect is the result of a non-diffusion microstructure changing characterized by a good reversibility at environmental temperature. Furthermore, the copper-based shape memory alloys are preferred for their good memory properties and low cost of production.
In this work, fatigue crack propagation and microstructural fracture micromechanisms are analyzed in order to identify microstructure influence on fatigue behavior of Cu-Zn-Al PE alloy.

SOMMARIO. I materiali a comportamento pseudo-elastico (PE) sono una importante classe di materiali che esibiscono una caratteristica unica nel panorama del materiali metallico, cioè quella di recuperare, alla temperatura ambiente, la forma iniziale anche a seguito di deformazioni molto elevate. Ciò è dovuto alla capacità di questi materiali di modificare, in modo completamente reversibile, la struttura cristallina di partenza secondo meccanismi non diffusivi come risposta a sollecitazioni meccaniche esterne. Tali trasformazioni sono completamente reversibili appena viene tolto il carico esterno.
In questo lavoro è stata osservata la propagazione della cricca di fatica di un provino CT. Le superfici di frattura sono state successivamente osservate al microscopio elettronico a scansione (SEM) per identificare i principali micro meccanismi di frattura.

KEYWORDS. Zn-Cu-Al alloy; Pseudoelastic behavior; Fatigue Crack Micromechanisms.

INTRODUCTION

Shape memory alloys (SMA) are the metallic alloys that exhibit a metallurgical phenomenon: the ability of alloys to recover an undeformed shape after high values of deformation. Some traditional SMA are equiatomic NiTi alloys and Cu-Zn-Al alloys. There are two different mechanical behaviors of SMA:

1) A shape memory effect (SME), when the recovery of the initial shape takes place only after heating over critical temperature, followed by a transition of crystallographic structure;
2) A psuedoelastic effect (PE), when the critical temperature is less than the environmental temperature. In this case the recovery of the initial shape takes place after unloading because physical conditions are able to perform a recovery of the initial crystallographic structure.

From the discovery of the first shape memory alloy (Au-Cd in 1938), many alloys, characterized by memory property, have been studied. Often the composition was characterized by the presence of rare metals and poor mechanical properties and effects that did not allow an industrial development on a large scale. In recent years, mechanical property of many SMA has improved in order to introduce these alloys in specific field of industry. Main examples of these alloys are the NiTi, Cu-Zn-Al and Cu-Al-Ni which are used in many fields of engineering such as aerospace or mechanical systems [1].
Many scientific papers are published mainly on NiTi alloy (Nitinol), covering both aspects of the microstructure and thermo-mechanical properties [2]. However, this alloy is characterized by some processing difficulties that imply an increase of costs. The main difficulty is due to presence of titanium that makes it readily oxidisable and because of its good mechanical properties it must be hot worked.
Cu-Zn-Al alloys are characterized by good shape memory properties due to a bcc disordered structure stable at high temperature called β-phase, which is able to change by means of a reversible transition to a B2 structure after appropriate cooling, and reversible transition from B2 secondary to DO3 order, under other types of cooling. In β-Cu-Zn-Al shape memory alloys, the martensitic transformation is not in equilibrium at room temperature. It is therefore often necessary to obtain the martensitic structure, using a thermal treatment at high temperature followed by quenching. The martensitic phases can be either thermally-induced spontaneous transformation, or stress-induced, or cooling, or stressing the β-phase. Direct quenching from high temperatures to the martensite phase is the most effective because of the non-diffusive character of the transformation. The martensite inherits the atomic order from the β-phase [3].
Precipitation of many kinds of intermetallic phases is the main problem of treatment on ùcu-based shape memory alloy. For instance, a precipitation of α-phase occurs in many low aluminum copper based SMA alloy and presence of α-phase implies a strong degradation of shape recovery [7]. However, Cu-Zn-Al SMA alloys characterized by aluminum contents less than 5% cover a good cold machining and cost is lower than traditional NiTi SMA alloys.
In order to improve the SMA performance, it is always necessary to identify the microstructural changing in mechanical and thermal conditions, using X-Ray analyses.
In this work a Cu-Zn-Al SMA alloy obtained in laboratory has been microstructurally and metallographically characterized by means of X-Ray diffraction and Light Optical Microscope (LOM) observation. These analysis have performed in "as cast alloy" and under load conditions in order to identify the behavior of alloy. Furthermore a fatigue crack propagation and fracture surface scanning electron microscope (SEM) observations have been performed in order to evaluate the main crack micromechanisms.

INVESTIGATED MATERIAL AND EXPERIMENTAL PROCEDURES

In this work a Cu-Zn-Al pseudo-elastic alloy, obtained by using an atmosphere controlled furnace and characterized by chemical composition shown in Table 1, has been used to investigate fatigue crack propagation.
From the melted alloy, under controlled atmosphere containing nitrogen gas, three castings occurred in the mold characterized by shape like CT specimen. Casting is driven by means of centrifugal force, whereas cooling is covered by environment conditions.

Cu	Zn	Al	Other
73.00	21.80	5.04	0.16

Table 1: Chemical composition of Cu-Zn-Al investigated alloy.

The crude specimens are machined in order to make CT specimens as ASTM E 647, and both lateral surfaces have been metallographically prepared to Light Optical Microscope (LOM) observations.
A traditional hydraulic testing machine has been used in order to evaluate fatigue crack propagation using the ASTM E 647 testing conditions.
Prior to evaluating fatigue behaviour pre-cracks of CT specimens using a crack rate $R=P_{min}/P_{max}=0.1$ have carried out until to get a crack rate lower than 10^{-12} m/cycle in order to evaluate the ΔK_{th} and $\Delta P_{th}=P_{max}-P_{min}$ corresponding to the threshold condition.
Fatigue cracks propagation is performed by using the following conditions:

1) $R=P_{min}/P_{max}=0.1$

2) $\Delta P=1.2\cdot\Delta P_{th}$ in the threshold conditions
3) Sinusoidal wave load
4) Load frequency=30Hz
5) Environmental temperature

Finally, fracture surfaces have been analysed by means of a Scanning Electron Microscope (SEM) in order to evaluate the main crack micromechanisms in different ΔK values.

EXPERIMENTAL RESULTS AND COMMENTS

LOM observations show a tradition structure whose grain diameter is about 700µm. Structure is not completely homogeneous and grains are characterized by a needle like morphology as shown in Fig. 1.

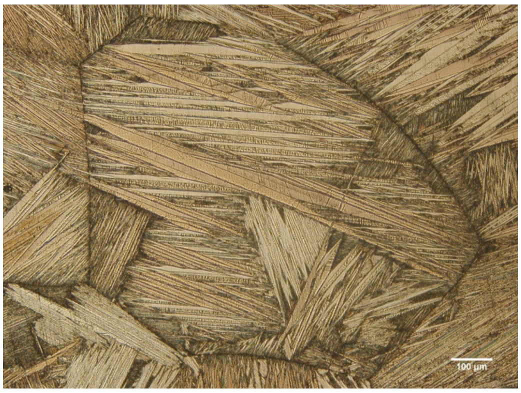

Figure 1: Etched surface of investigated material.

Needles structure are oriented with some covering the complete diameter of grains and others initiate at boundary grains and extend towards the needles' diameter. No subgrains are observed.
Fatigue crack propagation results are shown in Fig. 2 where five different stages can be observed. Two different kinds of alloy behavior can be observed in grouping stages 1, 2 and 3, and stages 3, 4 and 5.

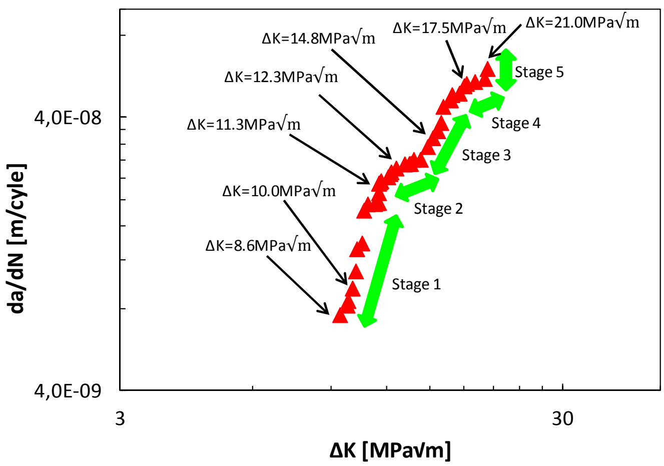

Figure 2: Fatigue crack propagation results (black arrows indicate the points observed in SEM analysis, green arrows indicate the different stages).

In particular the first group, containing stage 1, 2 and 3, can be attributed to the initial structure, but in stage 3 a structure transition takes place due to high values of ΔK.

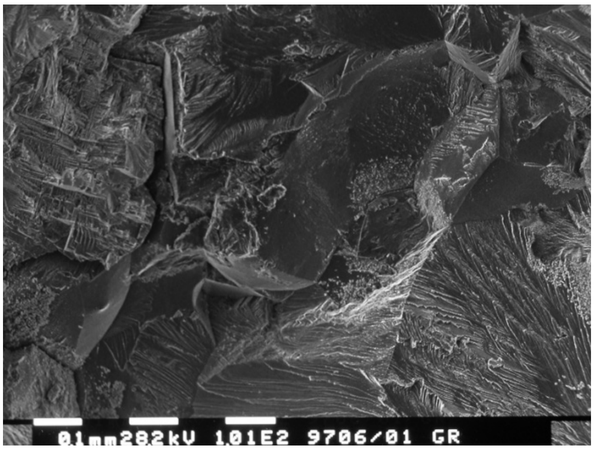

a)

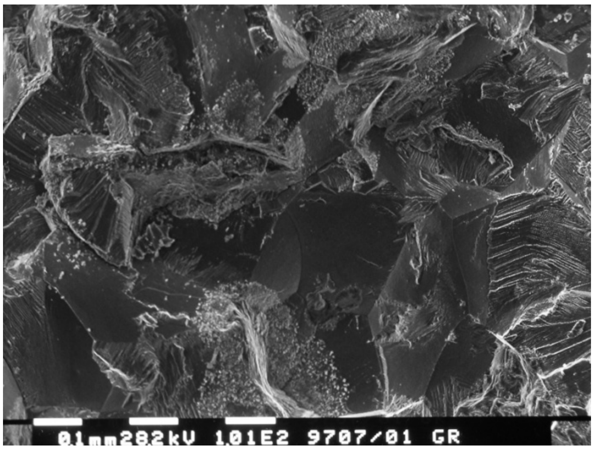

b)

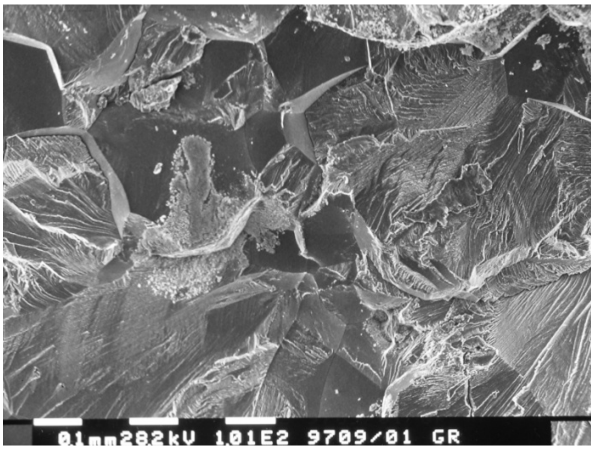

c)

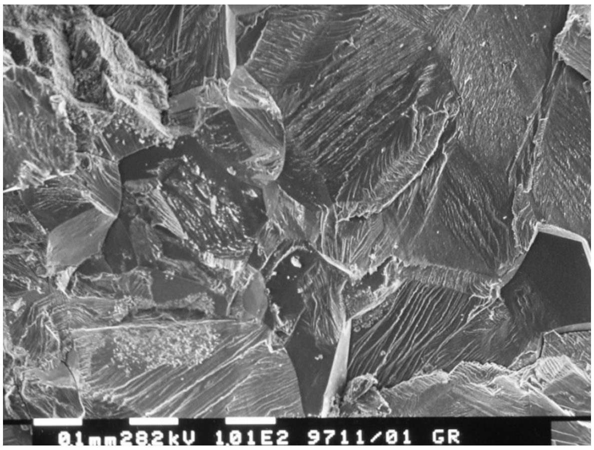

d)

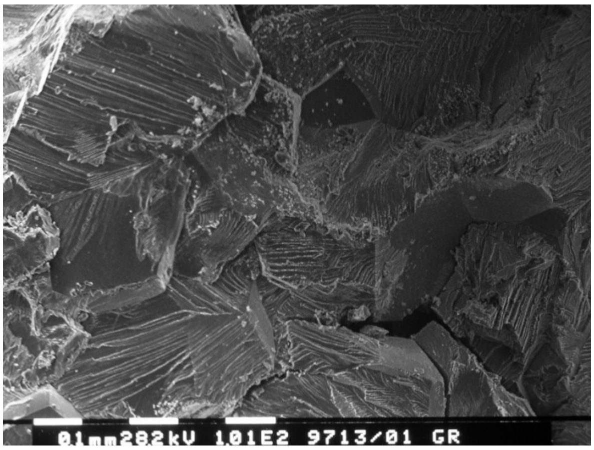

e)

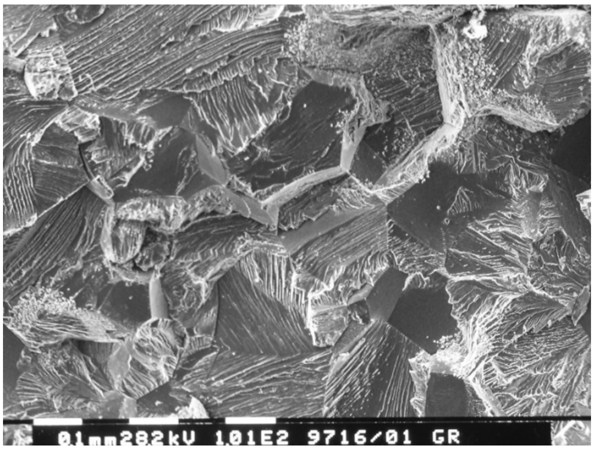

f)

Figure 3: Fracture surface at low and medium ΔK values: a) ΔK=8.6 MPa√m%, b) ΔK=10.0 MPa√m, c) ΔK=11.3 MPa√m, d) ΔK=12.3 MPa√m, e) ΔK=14.8 MPa√m, f) ΔK=17.5 MPa√m.

During the structure changing, stage 3 is characterized by a very linear correlation up to a complete transition to the new structure. From this point onwards, the material is characterized by a new behavior (stage 4) up to higher values of ΔK (stage 5), followed by instable propagation.

Fracture analyses show a presence of fatigue striation and intergranular/transgranular cleavage at low values of ΔK in stage 1 (as shown in Fig. 3a) and presence of fatigue striation and only intergranular cleavage at higher values of ΔK in stage 1. The sharp increase of crack rate that characterizes stage 1 can be attributed to presence of transgranular cleavage.
In the stage 2 presence of interganual cleavage and fatigue striation can be observed in Fig. 3c and 3d), but in these cases striation morphology are more oriented than striation of stage 1, and the distance between striation are greater.
Stage 3 is characterized by presence of intergranular cleavage and fatigue striations with presence o cracks due to debonding of grains, probable attributable to different grade of structure transition in the contiguous grains which generates different deformations (Fig. 3e).
In stage 4, the importance of fatigue striations increases (as shown in Fig. 3f).

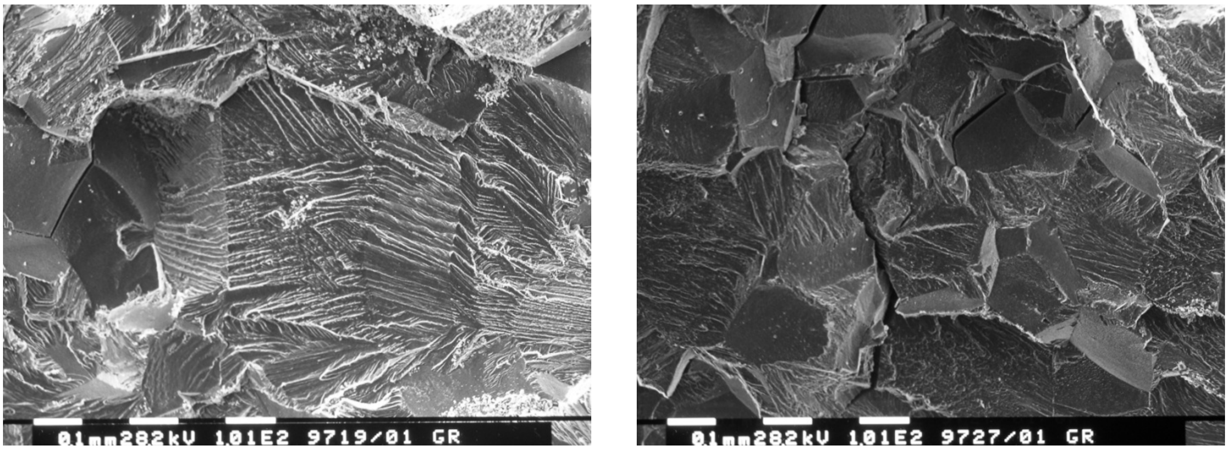

a) b)

Figure 4: Fracture surface at high ΔK values: a) ΔK=21.0 MPa√m, b) instable propagation.

At higher values of ΔK, near instable crack propagation conditions, the importance of striation increases and the values of the distance between striation increases. Furthermore fatigue striation morphology is more oriented along the main crack propagation (Fig. 4 a). However it is possible to see the presence of interganular cleavage characterized by secondary intergranular cracks up to instable conditions, where (Fig. 4c) secondary cracks propagate also in the zone characterized by presence of striations.

CONCLUSIONS

In this work, the fatigue crack propagation in an Cu-Zn-Al shape memory alloy, obtained in laboratory, has been evaluated in correlation to main crack micromechanisms by using Scanning Electron Microscopy. Fatigue crack propagation has been carried out by means of traditional hydraulic fatigue crack machine tests and CT specimens, at ΔP=constant, R=0.1 in environment conditions (ASTM E 647).
The ability for material to change its structure under load generates a particular fatigue crack propagation behavior characterized by five different stages of which the third stage at middle investigated ΔK, the changing of structure take place.
From the fracture analyses point of view the following conclusion can be carried out:

1) Presence of intergranular cleavage cracks generate the sharply increase of crack rate in the stage 1
2) Stage 2 is characterized by presence of intergranular cleavage and fatigue striation more oriented than striation in stage 1
3) Stage 3 is the stage where structure change takes place with presence of grains debonding probably due to different grains deforming
4) Stage 4 is characterized by the presence of increasing ostriation importance.
5) Also in stage 5 the importance of striation increases, with the presence of secondary cracks between grains characterized by cleavage crack morphology
6) Secondary cracks characterized the instable propagation at higher values of ΔK.

REFERENCES

[1] J. Ma, I. Karaman, R.D. Noebe, International Materials Reviews, 2010, 55(5) (2010) 257.
[2] K. Otsuka, X. Ren, Progress in Materials Science, (2005) 511.
[3] T. Suzuki, R. Kojima, Y. Fujii, A. Nagasawa, Acta Metall. 37 (1) (1989) 163.
[4] V. Di Cocco L. Tomassi, C. Maletta, S. Natali, Workshop IGF, Forni di Sopra (UD), Italia, (2012) 62.
[5] PowderCell 2.3 PulverdiffraktogrammeausEinkristalldaten und Anpassungexperimenteller Beugungsaufnahmen. Available at http://www.bam.de/de/service/publikationen/powder_cell.htm.
[6] R. Zengin, N. Kayal, Acta Physica Polonica A, 118 (4) (2010).
[7] Vanja Asanovic, Kemal Delijic, Nada Jaukovic, Scripta Materialia, 58 (2008) 599.